Research Journal of Applied Sciences 2 (1): 89-94, 2007

Heat Transfer Analysis of Different Types of Metal Hydrides in a Simple Geometric Storage Tank

Ayoub Kazim
Dubai Technology and Media Free Zone Authority, Dubai Knowledge Village,
P.O. Box 73000 Dubai, United Arab Emirates

Abstract: In this study, a general 3-D steady state heat transfer analysis on a simple 1mX1mX1m hydrogen storage tank using different types of metal hydrides namely $La_{0.95}Nd_{0.05}Ni_5$, LmNi(l) and $Zr(Fe_{0.75}Cr_{0.25})_2$ is carried out at hydrogen absorption rates of $n=10^{-2}$, $n=10^{-3}$ and $n=10^{-4}$ mol/hr. The results demonstrated the significance of a higher absorption rate and reaction enthalpy of the metal hydride on the temperature distribution within the storage tank. Furthermore, a±12% and a negligible variation in the alloys temperature would occur if the changes in the thermal conductivity of hydrogen and convection coefficient are changed by±0.1 W/m°C and±1 W m^{-2}°C, respectively.

Key words: Hydrogen storage, metal hydride, heat transfer, temperature distribution, heat generation, absorption rate

INTRODUCTION

Generally, there are three basic methods for storing hydrogen namely gas compression, liquefaction and chemical bounding known as metal hydrides, which are the principal method of bonding hydrogen chemically. The best candidate for storing hydrogen is proved to be through metal hydrides due to their potential of storing up to 7% of hydrogen by weight and with a recent reported storage capability of 70% and safety features in comparison to the conventional methods[1]. Therefore, developments in metal hydride technology showed that the alloys provide an excellent opportunity for hydrogen storage at high safety standards.

Hydrogen storage through metal hydrides is a rather complex process since it involves heat and mass transfer as well as fluid flow and chemical reaction. Therefore, the analysis associated with such storage system in terms of temperature and concentration distributions and optimization of hydride beds could be extremely difficult and time consuming. To date, many numerical analyses on metal hydrides have been performed. However, the works of Dogan *et al.*[1-4] were considered some of the most comprehensive studies performed.

Some of the above investigations were elaborative and illustrated the transport behavior of the metal hydrides under transient condition, which is considered to be extremely essential in visualizing the evolution of hydride formation in the reactor. However, it should be noted that there is a need to understand the overall influence of the thermophysical properties of metal hydrides and their absorption rates on the temperature distribution in a simple geometrically shaped storage tank and under steady state condition.

The objective of the current study is to perform a 3-D, steady state heat transfer analysis on a simple 1mX1mX1m hydrogen storage tank using different types of metal hydrides. Furthermore, various hydrogen absorption rates will be used in the analysis as well. In addition, this work will take into consideration the natural convection between the ambient air and the exterior surface of the steel cladding of the storage tank.

HEAT TRANSFER EQUATIONS

A 3-D steady state analysis will be conducted on a 1mX1mX1m storage tank depicted in Fig. 1. The tank is made of steel with a 5 cm thickness and a geometric symmetry can be applied. Although the thickness of the steel cladding is relatively small compared to length of the storage tank, the analysis will take into consideration coupling the heat transfer equations of the steel cladding (heat conduction) with the interior of the tank (heat conduction with heat generation). The tank properties are presented in Table 1.

Steel cladding: Assuming no heat generation in the layer and with constant properties, the 3-D energy equation of the steel cladding in rectangular coordinates and under steady state condition is[5]:

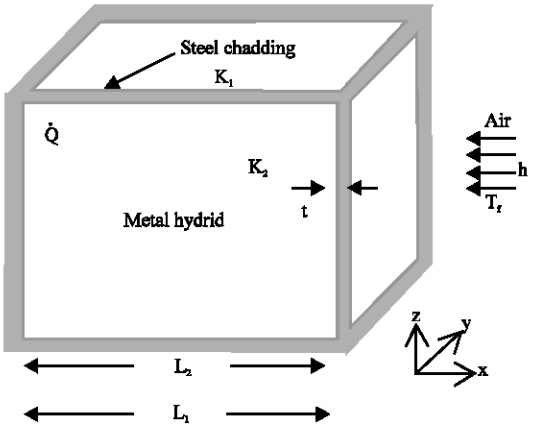

Fig. 1: Hydrogen storage tank

Table 1: Properties of metal hydrides and hydrogen storage tank[5,6]

Property	Quantity
Thermal conductivity of the steel cladding, k_1 (W/m °C)	15
Effective thermal conductivity of the metal hydride, k_2 (W/m °C)	0.6
Reaction of enthalpy (ΔH_{mh}) of $La_{0.95}Nd_{0.05}Ni_5$ (kJ/mol)	28.1
Reaction of enthalpy (ΔH_{mh}) of LmNi(l) (kJ/mol)	26.9
Reaction of enthalpy (ΔH_{mh}) of $Zr(Fe_{0.75}Cr_{0.25})_2$ (kJ/mol)	19.5
Convection heat transfer coefficient h (W/m² °C)	8
Film temperature T_f (°C)	25
Cladding thickness t (m)	0.05
Overall storage tank length with steel cladding, L_1 (m)	1
storage tank length without steel cladding, L_2 (m)	0.90

$$\frac{\partial^2 T}{\partial x^2}+\frac{\partial^2 T}{\partial y^2}+\frac{\partial^2 T}{\partial z^2}=0 \tag{1}$$

The boundary walls are assumed to be impermeable and no-slip conditions are valid at the boundary walls. The reaction heat is removed from the boundary walls with a cooling fluid of a temperature is T_f and a convection coefficient h. The corresponding boundary conditions are described in the following forms:

$$\begin{aligned}
&\text{At}\left(x=y=z=\frac{L_1}{2}=0.5\text{m}\right)\\
&-k_1\frac{\partial T}{\partial x}\left(\frac{L_1}{2},y,z\right)=h\left(T-T_f\right)\\
&-k_1\frac{\partial T}{\partial y}\left(x,\frac{L_1}{2},z\right)=h\left(T-T_f\right)\\
&-k_1\frac{\partial T}{\partial z}\left(x,y,\frac{L_1}{2}\right)=h\left(T-T_f\right)
\end{aligned} \tag{2}$$

$$\begin{aligned}
&\text{At}\left(x=y=z=\frac{L_2}{2}=0.45\text{m}\right)\\
&k_1\frac{\partial T}{\partial x}\left(\frac{L_2}{2},y,z\right)=k_2\frac{\partial T}{\partial x}\left(\frac{L_2}{2},y,z\right)\\
&k_1\frac{\partial T}{\partial y}\left(x,\frac{L_2}{2},z\right)=k_2\frac{\partial T}{\partial y}\left(x,\frac{L_2}{2},z\right)\\
&k_1\frac{\partial T}{\partial z}\left(x,y,\frac{L_2}{2}\right)=k_2\frac{\partial T}{\partial z}\left(x,y,\frac{L_2}{2}\right)
\end{aligned} \tag{3}$$

where k_1, k_2 are thermal conductivity of the steel cladding and thermal conductivity of the hydrogen inside the tank, respectively. Moreover, L_1 and L_2 represent the entire length of the storage tank and length of the tank without the steel cladding, respectively.

Metal hydride: Assuming constant properties, the basic 3-D energy equation inside the storage tank and under steady state condition is expressed as[5]:

$$\frac{\partial^2 T}{\partial x^2}+\frac{\partial^2 T}{\partial y^2}+\frac{\partial^2 T}{\partial z^2}+\frac{\dot{Q}}{k_2}=0 \tag{4}$$

where $\dot{Q}$ represents heat generation within the storage tank, which is a volumetric phenomena and it can be described with respect to reaction enthalpy of the metal hydride ΔH_{mh} and absorption rate denoted by n[6]:

$$\dot{Q}=\frac{\Delta H_{mh}\,n}{L_2^3} \tag{5}$$

where L_2 represents length of the tank without the cladding.

The above described heat generation within the tank is assumed to be constant and uniform as a result of insignificant pressure gradient within the hydride bed, which is mainly regarded to be sufficiently porous.

The corresponding boundary conditions can be described in the following forms:

$$\begin{aligned}
&\text{At}\left(x=y=z=0\right)\ \frac{\partial T}{\partial x}(0,y,z)=0\\
&\frac{\partial T}{\partial y}(x,0,z)=0\ \ \frac{\partial T}{\partial z}(x,y,0)=0\\
&\text{At}\left(x=y=z=\frac{L_2}{2}=0.45\text{m}\right)
\end{aligned} \tag{6}$$

$$k_1\frac{\partial T}{\partial x}\left(\frac{L_2}{2},y,z\right)=k_2\frac{\partial T}{\partial x}\left(\frac{L_2}{2},y,z\right)$$
$$k_1\frac{\partial T}{\partial y}\left(x,\frac{L_2}{2},z\right)=k_2\frac{\partial T}{\partial y}\left(x,\frac{L_2}{2},z\right) \quad (7)$$
$$k_1\frac{\partial T}{\partial z}\left(x,y,\frac{L_2}{2}\right)=k_2\frac{\partial T}{\partial z}\left(x,y,\frac{L_2}{2}\right)$$

The Eq. 7 are valid for all types of metal hydrides, except $\dot{Q}$ that differs from one alloy to another. In this work, three metals namely $La_{0.95}Nd_{0.05}Ni_5$, LmNi(1) and $Zr(Fe_{0.75}Cr_{0.25})_2$ are selected based on their reaction enthalpy ΔH_{mh}, which could greatly influence the overall outcomes. In order to assess the effect of absorption rates on the temperature distribution within the tank, the analysis will be conducted at various n particularly at n = 10^{-4}, 10^{-3} and 10^{-2} mol hr^{-1}. In addition, it should be pointed out that the main reason for selecting simple 1mX1mX1m geometry is to establish a general profile of temperature distribution of metal hydrides inside a simple geometrically-shaped storage tank rather than a cylindrical shape. In reality, the tank must have an empty space to allow the expansion of metal hydride during the hydrogenation process. Moreover, the volume of the hydride material is usually expected to increase as a result of hydriding and dehydriding cycles[6]. However, for the sake of simplicity, the analysis will be carried out without allocating any space for hydrogen expansion.

Although the thickness of steel cladding is small compared to the length of the storage tank, the analysis will take into account its effect on the overall results. Therefore, the 3-D temperature distribution will be performed and plotted using FEMlab through coupling the two domains namely the steel cladding and the metal hydride. Furthermore, the analysis will be carried out through using the properties of the three metal hydrides as well as thermophysical properties of the storage tank presented in Table 1.

RESULTS AND DISCUSSION

The temperature distribution of $La_{0.95}Nd_{0.05}Ni_5$ depicted in Fig. 2 shows a progressive variation in the magnitude as the absorption rate of hydrogen rises from n=10^{-4} mol hr^{-1} to n=10^{-2} mol hr^{-1}. For instance, a maximum variation of 1.1 °C in the temperature is occurred as a result of a minor heat generation formed at a hydrogen absorption rate of n=10^{-4} mol hr^{-1} illustrated in Fig. 2a. This variation in the temperature is considered to be marginal in comparison to maximum temperature variation of 11 °C and 111.3 °C corresponding to absorption rates of n=10^{-3} mol hr^{-1} and n=10^{-2} mol hr^{-1}, respectively.

Fig. 2: 3-D temperature distribution of $La_{0.95}Nd_{0.05}Ni_5$ at absorption rates of (a) n=10^{-4} (b) n=10^{-3} and © n=10^{-2} mol hr^{-1}

Definitely, temperature distribution of the alloy posed to be more prominent in the case of n=10^{-2} mol hr^{-1} shown in Fig. 2c as a result of a higher absorption rate leading to a higher volumetric heat generation within the tank.

The temperature variation through various sections of the storage tank can be clearly noticed in Fig. 3, which presents two sections of the tank namely at the quarter of the tank (z = y = ±0.25 m) and in the center of the tank (z = y = 0). Due to the symmetric nature of the currently investigated tank, the results

Fig. 3: Temperature change of $La_{0.95}Nd_{0.05}Ni_5$ at z=y=0 m (center) and z=y=±0.25 m

could also be interpreted in the y-axis as well as z-axis (i.e. z = x = ±0.25 m and z = x = 0). It is noted that the maximum temperature reached by the substance is 136.3°C at the center of the tank of x = y= z = 0, with a negligible change in the temperature of the steel cladding due to high thermal conductivity as opposed to thermal conductivity of the hydrogen inside the tank. In addition, the steel cladding was analyzed with the absence of heat generation throughout the medium in contrast to the interior of the tank, where heat generation is regarded to be essential.

Generally, the temperature rise occurs when we move toward the center of the tank and a temperature drop occurs as we move away from the center depicted in Fig. 3. For instance at an absorption rate of $n=10^{-2}$ mol hr^{-1} and z = y = ±0.25m, the temperature gradually rises from the initial point at x= -0.45 m to the center at x= 0, then decreases with the same proportion as a result of symmetry imposed in the analysis. A 27.5% increase in the temperature is detected between the quarter of the tank (x = 0, z = y = ±0.25 m) and the center of the tank (x=y=z = 0). Furthermore, the results indicate the negligible temperature variation in the steel cladding with the thickness range of $0 \le x \le 0.05$ m, illustrating the high thermal conductivity of the material. It should also be noted that the convection heat transfer contributed in an insignificant change on the exterior temperature of tank T_1, as a result of low convection coefficient used in the analysis indicating solely a free convection heat transfer.

With exception to the magnitudes of temperature variations, similar observations can be made concerning the other two metal hydrides namely LmNi(l) and $Zr(Fe_{0.75}Cr_{0.25})_2$, which are presented in Figures 4-7. The maximum temperature reached by LmNi(l) and $Zr(Fe_{0.75}Cr_{0.25})_2$ are 131.5°C and 102.2°C at the center of the tank of x= y= z= 0, respectively. The maximum temperature variation of LmNi(l) is estimated to be 106.5°C, which

Fig. 4: 3-D temperature distribution of LmNi(l) at absorption rates of (a) $n=10^{-4}$ (b) $n=10^{-3}$ and (c) $n=10^{-2}$ mol hr^{-1}

Fig. 5: Temperature change of LmNi(l) at z=y=0 m (center) and z=y= ±0.25 m

Fig. 6: 3-D temperature distribution of $Zr(Fe_{0.75}Cr_{0.25})_2$ at absorption rates of (a) $n=10^{-4}$ (b) $n=10^{-3}$ and (c) $n=10^{-2}$ mol hr^{-1}

occurs at $n=10^{-2}$ mol hr^{-1}. By the same token, the maximum temperature variation of $Zr(Fe_{0.75}Cr_{0.25})_2$ is estimated to be 77.2°C at the same absorption rate. Furthermore, Fig. 5 and 7 demonstrate a 27.2 and 25% increase in the temperature between the quarter of the tank (x=0, z = y = ±0.25m) and the center of the tank (x=y=z=0) of LmNi(l) and $Zr(Fe_{0.75}Cr_{0.25})_2$, respectively.

Heat generation which is defined in terms of the reaction enthalpy of the metal hydride ΔH_{mh} and hydrogen absorption flow rate n, is greatly influenced by these two

Fig. 7: Temperature change of $Zr(Fe_{0.75}Cr_{0.25})_2$ at z=y=0 m (center) and z=y= ±0.25 m

key parameters. However, n tends to be more influential than ΔH_{mh}, which is constant and it is associated with the type of the metal hydride used. For instance, the difference in the maximum temperature between $La_{0.95}Nd_{0.05}Ni_5$ and $Zr(Fe_{0.75}Cr_{0.25})_2$ that occurs in center of the tank (x = y = z = 0) is 34°C, which is 50% less than the difference between $n= 10^{-4}$ and $n=10^{-2}$ mol hr^{-1} of $Zr(Fe_{0.75}Cr_{0.25})_2$. Conversely, in the case of $La_{0.95}Nd_{0.05}Ni_5$, the difference between $n= 10^{-4}$ and $n=10^{-2}$ mol hr^{-1} is 70% more than the difference in the maximum temperature between $La_{0.95}Nd_{0.05}Ni_5$ and $Zr(Fe_{0.75}Cr_{0.25})_2$.

As reported by Vanhanen *et al.*[6] the convection coefficient of air and thermal conductivity of hydrogen in the storage tank could vary by±1 W/m^2 °C and±0.1 W/m °C. By taking these values into consideration, a±12% change in the temperature distribution would be anticipated if the thermal conductivity of hydrogen is changed by±0.1 W/m °C. In addition, a negligible ±0.004% change in the temperature distribution would be predicted if the convection coefficient is changed by±1 W/m^2 °C demonstrating the insignificance of free convection on the overall temperature distribution in the storage tank. Also, a±3.5% of temperature variation could occur in case if the cladding thickness is increased or lowered by 1 cm from the originally set thickness of 5 cm. Finally, it should be emphasized that the current performed analysis is quite simple in comparison to the real case where metal hydride beds for proficient operations in both the charging and discharging that requires analysis of complex mass and heat transfer procedures inside the hydride bed[1]. Nevertheless, the study provides a general trend of temperature distribution of metal hydrides with various absorption rates and at a simple geometric storage tank.

CONCLUSION

In this study, a 3-D, steady-state heat transfer analysis of a simple geometric hydrogen storage system

using different types of metal hydrides was performed at various hydrogen absorption rates. The results demonstrated that the reaction enthalpy of the metal hydrides and hydrogen absorption flow rate are the two key factors that could significantly affect the overall results with n to be more influential than ΔH_{mh}. Moreover, variation in the steel cladding's temperature tends to be negligible due to high thermal conductivity. However, temperature variation tends to be more prominent inside the tank as a result of low thermal conductivity and existence of heat generation. Finally, a±12% and a negligible variation in the alloys temperature would occur if the changes in the thermal conductivity of hydrogen and convection coefficient are changed by ±0.1 W/m °C and±1 W/m^2 °C, respectively.

Nomenclature:

h	Convection heat transfer, W/m^2 °C
Δh_{mh}	Reaction enthalpy of the metal hydride, kJ/mol
k_1	Thermal conductivity of the steel cladding, W/m °C
k_2	Effective thermal conductivity of the metal hydride, W/m°C
L_1	Entire length of the storage tank, m
L_2	Length of the tank without the steel cladding, m
$\dot{n}$	Hydrogen absorption flow rate, mol hr^{-1}.
$\dot{Q}$	Heat generation within the storage tank, W m^{-3}
t	Thickness, m
T	Temperature, °C
T_f	Fluid temperature, °C

REFERENCES

1. Dogan, A., Y. Kaplan and T.N. Nejat Veziroglu, 2004. Numerical investigation of heat and mass transfer in a metal hydride bed. Applied Mathematics and Computation. 150: 169-180.
2. Askri, F., A. Jemni and S. Ben Nasrallah, 2004. Prediction of transient heat and mass transfer in a closed metal–hydrogen reactor. International J. Hydrogen Energy, 29: 195-208.
3. Aldas, K., M.D. Mat and Y. Kaplan, 2002. A three-dimensional mathematical model for absorption in a metal hydride bed. International J. Hydrogen Energy, 27: 1049-1056.
4. Ben, S., Nasrallah and A. Jemni, 1997. Heat and mass transfer models in metal-hydrogen reactor. International J. Hydrogen Energy, 22: 67-76.
5. Cengel, Y. and M. Boles, 1994. Thermodynamics-an Engineering Approach. Mc Graw-Hill, Inc., 2nd Edn.
6. Vanhanen, J.P., P. Lund and M.T. Hagström, 1996. Feasibility study of a metal hydride hydrogen store for a self-sufficient solar hydrogen energy system. International J. Hydrogen Energy, 21: 213-221.